The spiralling self-avoiding walk in a random environment

1992 J. Phys. A: Math. Gen. 25 285

(http://iopscience.iop.org/0305-4470/25/2/012)

J. Phys. A: Math. Gen. **25** (1992) 285-301. Printed in the UK

The spiralling self-avoiding walk in a random environment

M Nifle and H J Hilhorst

Laboratoire de Physique Théorique et Hautes Energies†, Bâtiment 211, Université de Paris-Sud, 91405 Orsay, France

Received 12 July 1991

Abstract. We study the spiralling self-avoiding lattice walk in a random environment. Upon scaling the temperature appropriately with system size, a phase transition appears. In the low temperature phase the walk segments occupy a few low-energy positions, in the high-temperature phase they are effectively free. An analogy with the random energy model is pointed out. The average size of an N-step walk is shown to be asymptotically proportional to $N^{1/2}\log N$ (as was known for the homogeneous lattice), with a coefficient that increases as the temperature is lowered. The spatial distribution of the walk segments is qualitatively different above and below the critical temperature. The model also allows for a spin glass interpretation, and as such helps to clarify the connection between the concepts of frustration and the chaoticity of the pair correlation both above and below the critical point.

1. Introduction

The study of spiralling self-avoiding walks (SAWs) on a homogeneous lattice was initiated by Privman [1] in 1983. Such a walk, besides being self-avoiding, is subject to the constraint that, when traversed in a given sense, each step can only be either in the same direction as its predecessor, or rotated by $+\pi/2$ with respect to it. A typical spiralling SAW is shown in figure 1(a). It consists of both an outward and an inward

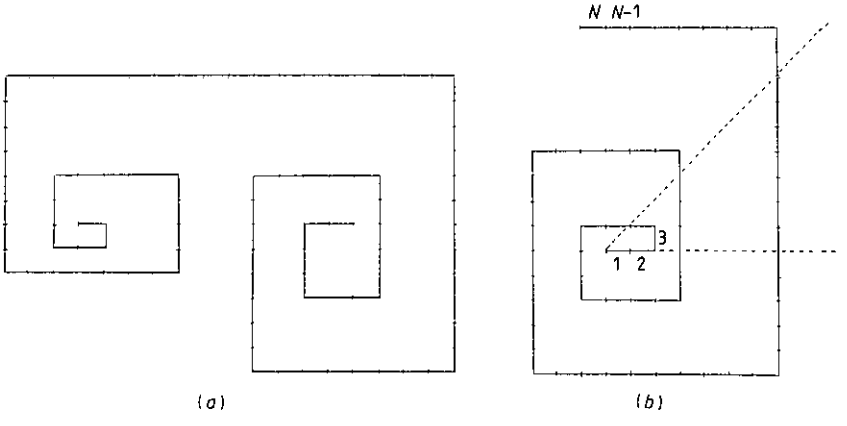

Figure 1. Two examples of N-step spiralling self-avoiding walks on a square lattice. (a) Typically, a spiralling SAW consists of an outward and an inward spiralling part. The two parts are statistically equivalent. (b) An outward spiralling SAW. Only this subclass of spirals is studied here. The dashed lines indicate a sector of $\pi/4$.

† Laboratoire associé au Centre National de la Recherche Scientifique.

0305-4470/92/020285+17$04.50

spiralling part. Since statistically these two parts are identical [2], it suffices to study only the class of outward spirals, of which a typical example is shown in figure 1(*b*).

Two of the questions asked for a spiral SAW are the same ones as for an ordinary SAW:

(i) what is the total number Z_n of N-step walks?

(ii) what is the root-mean-square end-to-end distance, $\langle R_N^2 \rangle^{1/2}$, of an N-step walk?

Analytic results for spiralling SAWs on a homogeneous square lattice were first obtained [2, 3] in 1984, and extended in various ways by several authors [4]. It was shown [2] in particular that for the class of outward spirals on a square lattice

$$Z_N \simeq 2^{-3/2}\pi^{-1}N^{-1/2}\exp(\pi\sqrt{2N/3}) \qquad (N\to\infty) \tag{1.1a}$$

$$\langle R_N^2 \rangle^{1/2} \simeq \tfrac{1}{2}\sqrt{3}\,\pi^{-1}N^{1/2}\log N \qquad (N\to\infty). \tag{1.1b}$$

In this work we shall study spiralling SAWs in a random medium. We shall ask how, as a function of temperature, the properties (1.1) of the spiralling walk are affected by the disorder.

On a lattice one introduces disorder by associating a random energy value with each link between neighbouring lattice points. The energy of a walk then is the sum of the energies of the links through which it passes. It is known, for example from studies [5, 6] of the directed self-avoiding walk, that disorder creates a tendency for the walk to extend in space: it tries to settle in low-energy regions, even though these are farther away from its origin.

On a random lattice the walk's properties become temperature dependent. In particular, in certain cases a transition may appear from a low temperature phase, where the walk is localized in a few low-energy regions ('valleys'), to a high-temperature phase where its large-scale behaviour is qualitatively the same as on a homogeneous lattice. The spiralling SAW studied in this paper, just like the directed walk in $1+1$ dimensions, is always in its low-temperature phase if one uses the standard temperature variable. We shall use, however, a temperature rescaled with system size, and as a consequence a phase transition appears.

The plan of the paper is as follows. In sections 2 and 3 we define the model and give expressions for its main properties in terms of the rescaled variables. In section 4 we characterize the phase transition and point out an approximate analogy between our model and the random energy model [7]. In section 5 we define a spin system equivalent to the spiralling SAW. We study the correlation between two spins and find that it varies chaotically with temperature. It is shown that frustration is at the origin of this chaoticity, just as it is in standard spin glass models [8]. The chaoticity of the pair correlation is characterized by an explicit expression for its density of zeros on the temperature axis. In section 6 we show the effect of randomness on the size of the SAW and comment upon the relative importance of thermal and of sample-to-sample size fluctuations. Section 7 contains a summary and perspectives, and may be read independently.

2. Simplified model of a spiral walk. Partition function and thermal averages

We shall describe the spiral walk by a simplified model which retains all the basic features. In a sector of $\pi/4$ of a square lattice (see figure 2) a number of vertical segments of integer heights are placed at integer positions, such that the sum of all

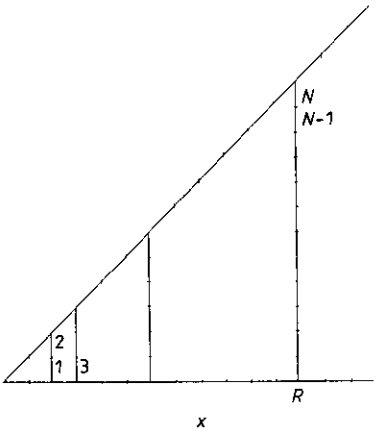

Figure 2. A sector of $\pi/4$ filled with vertical segments of a total length N.

segment heights is equal to N. The number of segments is not fixed. We identify the model of figure 2 with the sector of the spiralling walk between the dashed lines in figure 1(*b*). The idea behind this is that the dynamical variables of the full spiral walk (figure 1(*b*)) may be divided into two weakly coupled subsets, namely the position of the horizontal segments, and those of the vertical segments. The partition function of the full model will therefore be essentially the square of the partition function of the simplified model. One may verify this via a direct calculation following the method of [2]. In this work we shall content ourselves to show that quantities such as the size of the walk have, in the zero disorder limit, the same expression as found for the full model.

In order to study the model analytically we introduce occupation numbers n_x for $x = 1, 2, \ldots$, such that $n_x = 0$ and $n_x = 1$ correspond to the absence and the presence, respectively, of a vertical segment on site x. The randomness of the environment will be expressed by a random energy associated with each bond. The only combinations of variables entering the model are the sums of the energies in an entire vertical segment. Let ε_x denote the value of the sum of the x bond energies at site x. The Hamiltonian $\mathcal{H}$ then is

$$\mathcal{H} = \sum_{x=1}^{\infty} n_x \varepsilon_x. \tag{2.1}$$

We shall take the ε_x to be Gaussian distributed with mean zero and root mean square deviation $J\sqrt{x}$, where J sets the energy scale. It will also be useful to work with normalized dimensionless random variables u_x defined by

$$\varepsilon_x = J\sqrt{x}\, u_x \tag{2.2}$$

whose probability law is

$$p(u_x) = \frac{1}{\sqrt{2\pi}} e^{-\frac{1}{2}u_x^2}. \tag{2.3}$$

In the limit $J \to 0$ one recovers the homogeneous lattice.

The total number of bonds, N, and of segments, L, are given by

$$N = \sum_{x=1}^{\infty} x n_x \tag{2.4a}$$

$$L = \sum_{x=1}^{\infty} n_x. \tag{2.4b}$$

Let the system size R be defined as the position of the last segment. The expression for R in terms of the n_x then is

$$R = \sum_{x=1}^{\infty} x n_x \prod_{y=x+1}^{\infty} (1 - n_y). \tag{2.5}$$

Rather than calculating at fixed N, we shall introduce a chemical potential μ and calculate the grand-canonical partition function

$$\begin{aligned} Z(\beta, \mu) &= \sum_{\{n_x\}} \exp\left(-\beta J \sum_{x=1}^{\infty} \sqrt{x}\, n_x u_x + \beta\mu \sum_{x=1}^{\infty} x n_x \right) \\ &= \prod_{x=1}^{\infty} [1 + \exp(-\beta J \sqrt{x}\, u_x + \beta\mu x)] \end{aligned} \tag{2.6}$$

where β denotes the inverse temperature. Quantities of interest are the averages and fluctuations of the n_x and N, L, R and $\mathcal{H}$. From (2.6) one finds directly

$$\langle n_x \rangle = -\frac{1}{\beta J \sqrt{x}} \frac{\partial \log Z}{\partial u_x} = \frac{1}{1 + \exp(-\beta\mu x + \beta J \sqrt{x} u_x)} \tag{2.7}$$

where $\langle \ldots \rangle$ denotes the grand-canonical average. Equations (2.1), (2.4) and (2.7) allow one to write down immediately expressions for $\langle \mathcal{H} \rangle$, $\langle N \rangle$ and $\langle L \rangle$. In order to find $\langle R \rangle$, it suffices to note that in the grand-canonical ensemble the occupation numbers n_x are independent variables, and hence that

$$\langle n_x n_{x'} \rangle = \langle n_x \rangle \langle n_{x'} \rangle \qquad \text{for all } x \neq x'. \tag{2.8}$$

Therefore $\langle R \rangle$ is given by (2.5) but with all occupation numbers replaced by their averages. We still note the relation

$$\langle N^2 \rangle - \langle N \rangle^2 = \sum_{x=1}^{\infty} x^2 \langle n_x \rangle (1 - \langle n_x \rangle). \tag{2.9}$$

All the thermal averages calculated above depend on the disorder, that is, on the set $\{u_x\}$ of random parameters. In the next section we shall consider averages over the disorder.

3. Thermodynamic properties

3.1. Rescaling of temperature. The averages $\overline{\langle N \rangle}$ and $\overline{\langle L \rangle}$

We shall let an overbar $\overline{\ldots}$ denote the average over the random energies. The disorder averaged mean number of bonds $\overline{\langle N \rangle}$ is a function of β and μ. By inverting this relation one obtains μ as a function of β and $\overline{\langle N \rangle}$. In what follows we shall determine the relation between β, μ, and $\overline{\langle N \rangle}$ explicitly in the limit of large $\overline{\langle N \rangle}$, and from then on use $\overline{\langle N \rangle}$ rather than μ as a control parameter.

From (2.4*a*) and (2.7) one has

$$\overline{\langle N\rangle}=\sum_{x=1}^{\infty}\int_{-\infty}^{\infty}\frac{\mathrm{d}u}{\sqrt{2\pi}}\,\mathrm{e}^{-\frac{1}{2}u^2}\,\frac{x}{1+\exp(-\beta\mu x+\beta J\sqrt{x}\,u)}. \tag{3.1}$$

One sees that the thermodynamic limit $\overline{\langle N\rangle}\to\infty$ occurs when $\mu\uparrow 0$. It will appear that in this limit the spiral self-avoiding walk problem is non-trivial if we scale the inverse temperature β with μ according to

$$\beta=-\frac{b}{m}\mu \tag{3.2}$$

where b and m are positive constants that will acquire an individual meaning below. If in equation (3.1) one changes the summation variable x into

$$y=\frac{\mu^2}{j^2}x \tag{3.3}$$

one obtains

$$\begin{aligned}\overline{\langle N\rangle}&=\frac{\mu^2}{j^2}\sum_{y}\int_{-\infty}^{\infty}\frac{\mathrm{d}u}{\sqrt{2\pi}}\,\mathrm{e}^{-\frac{1}{2}u^2}\,\frac{y}{1+\exp((bJ^2/m)(y+u\sqrt{y}))}\\&\simeq\frac{J^4}{\mu^4}\Phi\left(\frac{bJ^2}{m}\right)\qquad\text{as }\mu\uparrow 0\end{aligned} \tag{3.4}$$

where the function Φ, analysed in appendix A, is defined by

$$\Phi(z)=\int_0^{\infty}\mathrm{d}y\,y\int_{-\infty}^{\infty}\frac{\mathrm{d}u}{\sqrt{2\pi}}\,\mathrm{e}^{-\frac{1}{2}u^2}\,\frac{1}{1+\exp z(y+u\sqrt{y}).} \tag{3.5}$$

To arrive at the second line of (3.4) we have used that for $\mu\uparrow 0$ the values of y become dense.

Equation (3.4) shows that $\overline{\langle N\rangle}$ diverges proportional to μ^{-4}, with a coefficient that depends on b/m. If inversely one takes $\overline{\langle N\rangle}$ rather than μ as the independent parameter, one can write

$$\mu=-m\overline{\langle N\rangle}^{-1/4} \tag{3.6}$$

with a coefficient m that also depends on b/m, that is, m becomes a function of b. From (3.6) and (3.4) one finds that $m(b)$ is the solution of

$$\frac{m^4}{J^4}=\Phi\left(\frac{bJ^2}{m}\right). \tag{3.7}$$

Equations (3.6) and (3.2) lead to

$$\beta=b\overline{\langle N\rangle}^{-1/4} \tag{3.8}$$

so that one sees that b is the rescaled inverse temperature. The main properties of the function $m(b)$ are derived in appendix A. It is shown in particular that m decreases monotonously from ∞ to $m(\infty)=(\frac{3}{4})^{1/4}J$ when b goes from 0 to ∞.

From (2.4) and (3.4) one sees that the expression for the disorder average of the mean number of segments, $\overline{\langle L\rangle}$, will differ from (3.4) by a factor $x=J^2y/\mu^2$ in the integrand. Hence we have

$$\overline{\langle L\rangle}\propto\frac{1}{\mu^2}\qquad\text{as }\mu\uparrow 0. \tag{3.9}$$

Similarly, we get the disorder average of the thermal fluctuations of N from (2.9). As this differs from $\overline{\langle N\rangle}$ by a factor x^2, one easily obtains its asymptotic behaviour

$$\overline{\langle N^2\rangle - \langle N\rangle^2} \propto \frac{1}{\mu^6} \qquad \text{as } \mu \uparrow 0. \tag{3.10}$$

Since $\overline{\langle N\rangle}$ is of order $1/\mu^4$, the distribution of the number of bonds is sharply peaked.

3.2. Thermodynamics

Having established how to scale the temperature and the chemical potential, we now complete our study of the thermodynamics. For the average of the grand potential Ω we have, in the notation of (3.4) and (3.5),

$$\begin{aligned}\bar{\Omega} &= -\beta^{-1}\,\overline{\log Z} \\ &= -\frac{J^2}{\beta\mu^2}\int_0^\infty \mathrm{d}y \int_{-\infty}^{\infty} \frac{\mathrm{d}u}{\sqrt{2\pi}}\, \mathrm{e}^{-\frac{1}{2}u^2} \log\left(\left(1+\exp\left(-\frac{bJ^2}{m}(y+u\sqrt{y}\right)\right)\right).\end{aligned} \tag{3.11}$$

Using the method of appendix A and introducing the dimensionless variable $a \equiv m/bJ^2$ one can transform this into

$$\bar{\Omega} = \frac{J^4 a}{2\mu^3}\left[\frac{\pi^2}{6}a + \log 2 + \sum_{k=0}^{\infty}\frac{(-1)^k}{2a+k}\right]. \tag{3.12}$$

The series in the above expression converges for all positive a, and hence $\bar{\Omega}$ is analytic at all temperatures. Whereas this would seem to indicate the absence of a critical temperature, we shall see in fact in the next section, when studying the density distribution of the walk segments, that the system does undergo a phase transition.

One may check, by comparing (3.12) with (3.4) and (A.2), that $\overline{\langle N\rangle} = -(\partial\bar{\Omega}/\partial\mu)_\beta$, as it should be. Similarly, one may obtain from the expression (3.12) the average of the energy $E \equiv \langle \mathcal{H}\rangle = J\partial\Omega/\partial J$ as

$$\bar{E} = \frac{J^4 a}{\mu^3}\left[\log 2 + \sum_{k=0}^{\infty}\frac{(-1)^k}{2a+k} + 2a\sum_{k=0}^{\infty}\frac{(-1)^k}{(2a+k)^2}\right]. \tag{3.13}$$

One sees that both $\bar{\Omega}$ and $\bar{E}$ are asymptotically proportional to $\overline{\langle N\rangle}^{3/4}$. From (3.13) one finds, by taking the limit $b\to\infty$, the average of the ground state energy E_{GS},

$$\bar{E}_{\mathrm{GS}} = -(\tfrac{4}{3})^{3/4}\,\overline{\langle N\rangle}^{3/4} J \tag{3.14}$$

where we used (3.6) and the fact that $m(\infty) = (\frac{3}{4})^{1/4}J$.

The entropy is obtained from (3.4), (A3), (3.12) and (3.13)

$$\begin{aligned}\bar{S} &= (\bar{E} - \bar{\Omega} - \mu\,\overline{\langle N\rangle}) \\ &= \frac{J^2}{2\mu^2}\left[\frac{\pi^2}{3}a + \log 2 + \sum_{k=0}^{\infty}\frac{(-1)^k}{2a+k} + a\sum_{k=0}^{\infty}\frac{(-1)^k}{(2a+k)^2}\right].\end{aligned} \tag{3.15}$$

It is strictly zero in the zero temperature limit, where $b\to\infty$ and hence $a\to 0$.

3.3. The high temperature limit

In the limit $b\to 0$ the disorder should no longer have any effect and we should recover known results [2]. With the aid of the asymptotic behaviour of the function $\Phi(z)$ found

in appendix A (equation (A4a)), and using (3.2), one obtains from (3.4) after taking the limit $b \to 0$

$$\overline{\langle N \rangle} \simeq \frac{\pi^2}{12\beta^2\mu^2} \qquad (\beta \to 0). \tag{3.16}$$

This limit ($b \to 0$) is also the limit of vanishing disorder as one can check by using (3.1) in the limit $J \to 0$.

This asympotic expression for $\overline{\langle N \rangle}$, and the expression for $\overline{\langle L \rangle}$ that one can find similarly, can be shown to be identical to those of Blöte and Hilhorst [2], in whose notation $4N$, $2L$, and ε play the role of our $\overline{\langle N \rangle}$, $\overline{\langle L \rangle}$ and $-\beta\mu$, respectively. This observation establishes the equivalence, at least for these global features, of the models of figure 1(b) and figure 2. Comparison of (3.6) and (3.16) shows that in the limit $b \to 0$ a crossover takes place in the relation between μ and $\overline{\langle N \rangle}$.

3.4. The zero temperature limit

In the zero temperature ($b \to \infty$) limit the inner integrand in (3.5) is equal to unity if $u < -\sqrt{y} = -m(\infty)J^{-1}\overline{\langle N \rangle}^{-1/4}\sqrt{x}$ and to zero otherwise. The interpretation is that at zero temperature, at a distance x from the origin, all levels up to the local 'Fermi level' $-m(\infty)J\overline{\langle N \rangle}^{1/2}\sqrt{x}$ are filled, and all others are empty. Transforming back to the original variables with the aid of (3.6) and (2.2) we see that the Fermi level at site x is

$$\varepsilon_{F,x} = \mu x \tag{3.17}$$

i.e. an energy μ per bond.

Evaluation of (3.5) in the zero temperature limit gives

$$\Phi(\infty) = \int_0^\infty \mathrm{d}y\, y \int_{-\infty}^{-\sqrt{y}} \frac{\mathrm{d}u}{\sqrt{2\pi}} \mathrm{e}^{-\frac{1}{2}u^2} = \tfrac{3}{4} \tag{3.18}$$

in agreement with the alternative calculation of appendix A, equation (A4c). Hence eq. (3.5) becomes

$$\overline{\langle N \rangle} \simeq \frac{3J^4}{4\mu^4}. \tag{3.19}$$

In the following sections we shall set $J = 1$ in order to simplify the notation.

4. Phase transition and segment density

4.1. Spatial density of the spiral segments

Even though the N dependence of the size of the spiral at high and at low temperature is the same, we shall see that the system undergoes a phase transition at a critical temperature $b = b_c$. In order to show this, we calculate the disorder average of the occupation probability $\langle n_x \rangle$. Scaling the spatial coordinate according to

$$x = r\overline{\langle N \rangle}^{1/2} \tag{4.1}$$

and setting $J = 1$, the quantity to calculate becomes

$$\overline{\langle n(r) \rangle} = \int_{-\infty}^{\infty} \frac{\mathrm{d}u}{\sqrt{2\pi}} \mathrm{e}^{-\frac{1}{2}u^2} \frac{1}{1 + \exp(bm(b)r + b\sqrt{r}\,u)}. \tag{4.2}$$

For fixed b evaluation is possible for asymptotically large r (see appendix B). The result is that in the large-r limit

$$\overline{\langle n(r)\rangle} \simeq e^{-\kappa(b)r} \qquad \text{when } m(b) > b \tag{4.3a}$$

$$\overline{\langle n(r)\rangle} \simeq C_1(b)\frac{e^{-\kappa(b)r}}{\sqrt{2\pi r}} \qquad \text{when } m(b) < b \tag{4.3b}$$

where

$$\kappa(b) = bm(b) - \tfrac{1}{2}b^2 \qquad \text{if } m(b) > b \tag{4.4a}$$

$$\kappa(b) = \tfrac{1}{2}m^2(b) \qquad \text{if } m(b) < b \tag{4.4b}$$

and

$$C_1(b) = \frac{\pi}{b}\operatorname{cosec}\left(\pi\frac{m(b)}{b}\right). \tag{4.4c}$$

Since $m(b)$ is a decreasing function of b, the conditions $m(b) < b$ and $m(b) > b$ indicate a low-temperature ($b > b_c$) and a high-temperature ($b < b_c$) phase, respectively.

Hence (4.4) show that there is a phase transition between two phases of different asymptotic segment densities. The inverse critical temperature b_c is the solution of

$$m(b_c) = b_c. \tag{4.5}$$

We find from (4.5), (3.7) and (A.4b), upon restoring J, that it is given by

$$b_c J = \Phi^{1/4}(1) = 2^{1/4}. \tag{4.6}$$

The inverse decay length $\kappa(b)$ is a decreasing function of b, bounded by the two constants

$$\kappa(0) = \tfrac{1}{6}\pi\sqrt{3} = 0.907 \tag{4.7a}$$

$$\kappa(\infty) = \tfrac{1}{4}\sqrt{3} = 0.433 \tag{4.7b}$$

and taking the value $\kappa(b_c) = \tfrac{1}{2}\sqrt{2} = 0.707$ at criticality. In view of (4.3), for fixed large enough r the segment density *increases* when the temperature is *lowered*. Since the average total number of bonds, $\overline{\langle N\rangle}$, is fixed, the segment density necessarily goes down for smaller values of r, as can be verified explicitly. We see, therefore, that just as in other problems of SAWs in a random environment, the disorder increases the size of the walk, even though in the present case there is no change of critical exponents, but only of the coefficient (see section 6).

4.2. Higher moments of the spatial density

We can also derive the asymptotic behaviour of all moments $\overline{\langle n(r)\rangle^k}$. They are easy to obtain by a calculation similar to the one of appendix B for $k = 1$. For each k there appears to be a critical temperature b_k which is the solution of

$$m(b_k) = kb_k \tag{4.8}$$

and the asymptotic behaviour is given by

$$\overline{\langle n(r)\rangle^k} \simeq \overline{\langle n(r)\rangle}^k \qquad \text{when } b < b_k \tag{4.9a}$$

$$\overline{\langle n(r)\rangle^k} \simeq C_k(b)\frac{e^{-m^2(b)r/2}}{\sqrt{2\pi r}} \qquad \text{when } b > b_k \tag{4.9b}$$

where

$$C_k(b) = \int_{-\infty}^{\infty} dv \frac{e^{m(b)v}}{(1+e^{bv})^k} = \frac{1}{b} \frac{\Gamma(k-m/b)\Gamma(m/b)}{\Gamma(k)}. \tag{4.10}$$

The critical point b_k is smaller as k goes up. In the low-temperature region $\overline{\langle n(r)\rangle^k}$ is much larger than $\overline{\langle n(r)\rangle}^k$, and in the high-temperature region they are equal to leading order. This recalls similar results for the moments of the partition function of spin-glass models like the Sherrington–Kirkpatrick model [8] or the random energy model (REM) [7]. The analogy with the REM will be discussed further in subsection 4.4.

4.3. Localization of the segments below the critical temperature

A different analysis, again in the limit of large r, allows us to characterize the phase transition by means of an order parameter. Equation (4.2) shows that at large r, hence large x, a site x with an energy u is occupied by a segment of the walk with a probability close to 1 when $u < -m(b)\sqrt{r}$, and with a probability close to 0 when $u > -m(b)\sqrt{r}$. When the temperature decreases, the energy level $-m(b)\sqrt{r}$ goes up, and the number of sites almost certainly occupied will increase. Hence the walk will become more and more trapped at these low energy sites. We shall let $\Psi_r(b)$ denote the fraction of all segments at a distance $\sim r$ from the origin that are trapped at energies less than $-m(b)\sqrt{r}$. Hence

$$\Psi_r(b) = \left(\int_{-\infty}^{-m(b)\sqrt{r}} \frac{du}{\sqrt{2\pi}} e^{-\frac{1}{2}u^2} \langle n(r)\rangle \right) \Big/ \left(\int_{-\infty}^{\infty} \frac{du}{\sqrt{2\pi}} e^{-\frac{1}{2}u^2} \langle n(r)\rangle \right) \tag{4.11}$$

where $\langle n(r)\rangle$ is given by (2.7) and the rescaling (4.1). The denominator in (4.11) is equal to (4.2) and (4.3), in the limit of large r. The numerator is easily evaluated by the same methods. Upon defining

$$\Psi(b) = \lim_{r\to\infty} \Psi_r(b) \tag{4.12}$$

one finds

$$\Psi(b) = 0 \qquad \text{if } b < b_c \tag{4.13a}$$

$$\Psi(b) = \left(\int_{-\infty}^{0} dw\, e^{wm(b)/b} (1+e^w)^{-1} \right) \Big/ \left(\int_{-\infty}^{\infty} dw\, e^{wm(b)/b} (1+e^w)^{-1} \right)$$

$$= \pi^{-1} \sin \frac{\pi m(b)}{b} \sum_{k=0}^{\infty} \frac{(-1)^k}{k + m(b)/b} \qquad \text{if } b > b_c \tag{4.13b}$$

for the high and the low temperature phase, respectively (see ref [9], equations (3.311.2) and (3.311.9)). The low temperature phase is characterized, therefore, by a finite fraction of frozen segments in the large-distance limit. One easily finds that

$$\begin{aligned} &\Psi(b) \propto b - b_c \qquad \text{as } b \downarrow b_c \\ &\Psi(\infty) = 1. \end{aligned} \tag{4.14}$$

4.4. Similarity to random energy model

There is a qualitative similarity between the spiral SAW problem of this paper and the randon energy model (REM) [7]. The typical distance between two neighbouring

segments is $\overline{\langle n_x \rangle}^{-1}$. Hence, for large x a segment is far away from its neighbours, and can choose among a large number of sites with energy values having a Gaussian distribution. If a segment had a fixed number of sites attributed to it, it would be exactly equivalent, in the limit $r \to \infty$, to a REM. In reality, the segments have a weak interaction between them, which accounts for the differences with the REM. In particular, in our model the entropy (3.15) in the low-temperature phase is not strictly zero as it is in the REM.

The REM has a low-temperature phase with many coexisting pure states. One may therefore ask if pure states can be distinguished also in the spiral SAW model, how many there are, and what their energy and overlap distributions are. Similar questions were asked recently by Mézard [6] for the case of the directed walk, but we shall not address these issues here.

5. Chaotic correlation functions in the frozen phase

5.1. Spin glass interpretation of the model

The most interesting correlation effects appear if instead of the SAW interpretation of the Hamiltonian (2.1) we adopt a spin glass picture. In this interpretation there is a magnetic spin on each site of the dual lattice. The vertical segments are part not of a single spiral as in figure 2, but each is part of a different rectangular closed contour, the set of contours being completely nested, as shown in figure 3. We imagine that whenever a contour is put in place or taken away, the region of spins inside it is completely reversed with respect to the region outside it. Hence the spins in an area between two successive contours are fully correlated, and our interest is in correlations between spins separated by a distance larger than the average distance between the contours.

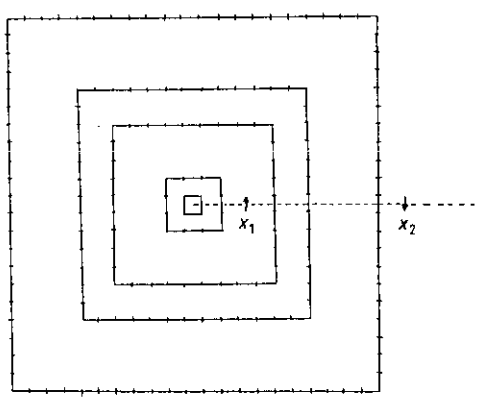

Figure 3. A set of nested contours on a lattice of magnetic spins.

Two Ising spins s_{x_1} and s_{x_2} (with x-coordinates $x_1+\frac{1}{2}$ and $x_2+\frac{1}{2}$, respectively, see figure 3) will therefore have a correlation

$$\langle s_{x_1} s_{x_2} \rangle_b = s^0_{x_1} s^0_{s_2} \langle (-1)^{n_{x_1+1}+\ldots+n_{x_2}} \rangle_b \tag{5.1}$$

where we have indicated explicitly the dependence of the thermal averages on the inverse temperature b. The product $s^0_{x_1} s^0_{x_2}$ is the reference value in the state without any contour, and we shall set it equal to unity for convenience.

5.2. Correlation length and chaotic temperature dependence

The correlation function (5.1) can also be written as

$$\langle s_{x_1} s_{x_2} \rangle_b = \prod_{y=x_1+1}^{x_2} (1-2\langle n_y \rangle_b). \tag{5.2}$$

We may express this as a product of two factors of which one will give the sign of the correlation and the other will contain the correlation length

$$\langle s_{x_1} s_{x_2} \rangle = (-1)^{\mathcal{N}_u(b)} \, \mathrm{e}^{-(x_2-x_1)/\xi_u(b)} \tag{5.3}$$

in which

$$(x_2-x_1)/\xi_u(b) + \mathrm{i}\pi \mathcal{N}_u(b) \equiv \lim_{\eta \downarrow 0} \sum_{y=x_1+1}^{x_2} \log\,[1-2\langle n_y \rangle_{b+\mathrm{i}\eta}] \tag{5.4}$$

where the index u is a reminder of the dependence on the disorder variables. We shall discuss successively the quantities ξ_u and $\mathcal{N}_u$. For x_1 and x_2 both of order $\overline{\langle N \rangle}^{1/2} r$ and $x_2 - x_1$ large, $\xi_u^{-1}(b)$ is self-averaging and approaches the inverse correlation length,

$$\bar{\xi}^{-1}(b) \equiv \int_{-\infty}^{\infty} \frac{\mathrm{d}u}{\sqrt{2\pi}} \, \mathrm{e}^{-\frac{1}{2}u^2} \log \tanh \tfrac{1}{2}[bm(b)r + bu\sqrt{r}]. \tag{5.5}$$

This quantity still depends on the distance r from the origin, and is therefore actually a local correlation length. Since two spins between the same pair of successive contours are completely correlated, it makes sense to define a correlation length $\Xi(b)$ on the length scale of the typical contour distance,

$$\Xi(b) = 2\overline{\langle n \rangle} \, \bar{\xi}^{-1}(b) \tag{5.6}$$

where the factor 2 is for later convenience. The integral in (5.5) can be evaluated, in the limit of large r, by the method of appendix A. Again the regimes $b > b_c$ and $b < b_c$ have to be distinguished. The result is that, for large r, $\Xi(b)$ tends to a constant value

$$\Xi(b) = 1 \qquad \text{if } b < b_c \tag{5.7a}$$

$$\Xi(b) = \left(\int_{-\infty}^{\infty} \mathrm{d}v \, \mathrm{e}^{vm(b)/b} (1+\mathrm{e}^v)^{-1} \right) \Big/ \left(\int_{-\infty}^{\infty} \mathrm{d}v \, \mathrm{e}^{vm(b)/b} \log|\tanh \tfrac{1}{2}v|^{-1/2} \right) \qquad \text{if } b > b_c. \tag{5.7b}$$

One easily verifies that the correlation length $\Xi(b)$ is continuous at $b = b_c$, and that it diverges as $\Xi(b) \sim b$ in the zero temperature ($b \to \infty$) limit. The result (5.7a), which refers to the high-temperature phase, is the same as would result if, at a given segment density $\langle n(r) \rangle_b$, all segments would move freely and randomly along the x axis. The increase of the correlation length (5.7b) below the critical temperature has the same cause as the appearence in section 4 of a non-zero order parameter: below criticality, segments gradually begin to freeze into a small number of fixed, randomly located, positions. A frozen segment at a site y corresponds to $\langle n_y \rangle = 1$, which in view of (5.1) contributes a factor -1 to the correlation, but does not contribute to the decay of its absolute value.

We turn now to the discussion of $\mathcal{N}(b)$ in (5.4). This quantity is equal to the number of sites y between x_1 and x_2 such that $\langle n_y \rangle > \frac{1}{2}$, or, equivalently, $u_y < -m(b)\sqrt{r}$. Since for $r \to \infty$ (and y of order $\overline{\langle N \rangle}^{1/2} r$) the average density $\langle n_y \rangle$ can only take the values 0

or 1, the quantity $\mathcal{N}(b)$ represents the number of frozen segments on the interval between x_1 and x_2. Its average value is

$$\bar{\mathcal{N}}(b) = (x_2 - x_1) \int_{-\infty}^{-m(b)\sqrt{r}} \frac{du}{\sqrt{2\pi}} e^{-\frac{1}{2}u^2}. \tag{5.8}$$

As the temperature is lowered, the set of sites occupied by a frozen segment can only increase. Therefore $d\mathcal{N}(b)/db$ represents the *density of sign changes on the temperature axis* of the correlation function $\langle s_{x_1} s_{x_2} \rangle_b$. It makes again sense to express $x_2 - x_1$ as a multiple of the intersegment distance via $x_2 - x_1 \equiv X\overline{\langle n(r) \rangle}^{-1}$. Using (5.8) and the explicit expressions (4.3) for $\overline{\langle n(r) \rangle}$ we obtain for the average density of sign changes

$$\rho(b) = X \frac{r}{C(b)\sqrt{2\pi}} \left| \frac{dm(b)}{db} \right| \qquad b > b_c \tag{5.9a}$$

$$= X \sqrt{\frac{r}{2\pi}} e^{-\frac{1}{2}(m(b)-b)^2 r} \left| \frac{dm(b)}{db} \right| \qquad b < b_c. \tag{5.9b}$$

Hence in the large-r limit, the density of sign changes for fixed spin separation tends to infinity in the low temperature phase (5.9a) and to zero in the high-temperature phase (5.9b). With increasing spin separation X the density increases without bound. Hence for a given temperature change Δb, the correlation function will undergo an arbitrarily large number of sign changes, which is the defining characteristic of *chaotic temperature dependence* [10].

The relation between disorder, frustration and chaotically temperature dependent correlations is now clear in this model. The Hamiltonian (2.1) is frustrated because, at a fixed number of bonds $\overline{\langle N \rangle}$, one cannot minimize each of its terms separately, and the minimum total free energy is the result of a compromise. Furthermore, imposing the constraint of a fixed $\overline{\langle N \rangle}$ in section 3 has rendered the chemical potential temperature dependent: $\mu = -m(b)\overline{\langle N \rangle}^{-1/4}$. We now see that in both equations (5.9) there is a factor $|dm(b)/db|$ present, so that the frustration is directly responsible for the chaotic correlations. Furthermore the relation between the chaotic behaviour and the phase transition appears.

Both above and below criticality the density of zeros increases indefinitely with the spin separation X. In the high-temperature phase, however, the correlation decays rapidly for $X > 1$, so that on those lengths scales the thermal effects are more important than the frustration. In the low-temperature phase, the correlation decays only when $X > \Xi(b)$, with $\Xi(b)$ going to infinity as temperature goes to zero. Hence there is an increasingly large spatial scale on which the chaoticity becomes important and will dominate physical properties such as relaxation times.

6. End-to-end distance of the SAW

The question we are interested in is to determine the effect of the disorder on the size of the spiralling SAW or, in our description in terms of segments, on the position R of the last segment. The same question has been answered for the directed polymer whose typical extension was found to increase due to the disorder. The result here is that the random medium does not modify the N dependence that we have given in (1.1b) for the homogeneous case, but only introduces a temperature dependent coefficient.

We obtain exactly the quantity $\overline{\langle R \rangle}$. Compared to (1.1*b*), the disorder has increased the size of the spiralling walk in agreement with our conclusion of section 4. We give a few comments about both thermal and sample-to-sample fluctuations of R at the end of this section.

From (2.5) and (2.8), one has for the average of the pth moment of the end-to-end distance

$$\overline{\langle R^p \rangle} = \sum_{x=1}^{\infty} x^p \overline{\langle n_x \rangle} \prod_{y=x+1}^{\infty} (1 - \overline{\langle n_y \rangle}) \tag{6.1}$$

where the exponent p will be equal to one or two. We scale the inverse temperature according to (3.8) and change the position variables x and y into

$$r = \frac{\mu^2}{\lambda_\mu} x \tag{6.2a}$$

$$r' = \frac{\mu^2}{\lambda_\mu} y. \tag{6.2b}$$

Here λ_μ is a scale factor yet to be determined, but we shall anticipate that it diverges as μ decreases to zero.

In the small-μ limit (6.1) becomes

$$\overline{\langle R^p \rangle} = \left(\frac{\lambda_\mu}{\mu^2}\right)^p \int_0^\infty \mathrm{d}r\, r^p\, \overline{\langle n(\lambda_\mu r) \rangle} \exp\left[-\frac{\lambda_\mu}{\mu^2} \int_r^\infty \mathrm{d}r'\, \overline{\langle n(\lambda_\mu r') \rangle} \right] \tag{6.3}$$

where we have exponential $1 - \overline{\langle n_y \rangle} \simeq \mathrm{e}^{-\overline{\langle n(\lambda_\mu r') \rangle}}$. We introduce the new variable of integration

$$s = \frac{\lambda_\mu}{\mu^2} \int_r^\infty \overline{\langle n(\lambda_\mu r') \rangle}\, \mathrm{d}r' \tag{6.4}$$

and we get

$$\overline{\langle R^p \rangle} = \left(\frac{\lambda_\mu}{\mu^2}\right)^p \int_0^\infty \mathrm{d}s\, r^p(s)\, \mathrm{e}^{-s} \tag{6.5}$$

we use (4.3) in (6.4) and find in the large $-\lambda_\mu$ limit

$$s \simeq \frac{1}{\mu^2 \kappa(b)} \overline{\langle n(\lambda_\mu r) \rangle}. \tag{6.6}$$

The scale λ_μ is determined by the condition that the main contribution to the integral (6.5) come from r' and s values that remain of order one as $\mu \to 0$. This gives

$$\lambda_\mu = \log |\mu|^{-1} \tag{6.7}$$

and to leading order r is given by

$$r = \frac{2}{\kappa(b)}. \tag{6.8}$$

The final result, upon integrating, is

$$\overline{\langle R^p \rangle} = \left(\frac{2}{\kappa(b)} \frac{\log |\mu|^{-1}}{\mu^2} \right)^p. \tag{6.9}$$

If one takes $\overline{\langle N\rangle} = m^4/\mu^4$, one gets in the $p=1$ case

$$\overline{\langle R\rangle} = \frac{1}{2\kappa(b)m^2(b)}\,\overline{\langle N\rangle}^{1/2}\log\overline{\langle N\rangle}. \tag{6.10}$$

The homogeneous case may be obtained upon taking the $J=0$ limit of (2.7) in (6.1). Then one takes $\langle N\rangle = \pi^2/12\beta^2\mu^2$ and finds again (1.1b). This is again the result for the full spiral (figure 1b) after the substitution indicated in section 3.3.

This calculation allows us to find an expression for $\langle R^2\rangle - \overline{\langle R\rangle}^2$. We need the following orders of $\langle R^p\rangle$ whose leading order is given by (6.9). This can be calculated immediately upon using the expansion of $r(s)$

$$r = \frac{2}{\kappa(b)} - \left(\frac{1}{2\kappa(b)}\frac{\log\log|\mu|^{-1}}{\log|\mu|}\right)^{\alpha} - \frac{\log(\kappa(b)s)}{\kappa(b)\log|\mu|^{-1}} \tag{6.11}$$

where $\alpha = 1$ when $b > b_c$ and $\alpha = 0$ otherwise. We find that the first orders vanish and get

$$\overline{\langle R^2\rangle} - \overline{\langle R\rangle}^2 = \frac{1}{\mu^4\kappa(b)}\left(\frac{\pi^2}{6} - 2C\log\kappa(b)\right) \tag{6.12}$$

where C is Euler's constant, and $\kappa(b)$ is given by (4.4) in both temperature regions. The quantity (6.12) therefore scales as $\overline{\langle N\rangle}$. Upon writing

$$\overline{\langle R^2\rangle} - \overline{\langle R\rangle}^2 = \overline{(\langle R^2\rangle - \langle R\rangle^2)} + \overline{(\langle R\rangle^2 - \overline{\langle R\rangle}^2)} \tag{6.13}$$

one sees that it is the sum of the thermal fluctuations (averaged over all samples), and the sample-to-sample fluctuations. Hence either of these is at most of order $\overline{\langle N\rangle}$. Since $\overline{\langle R^2\rangle}$ is of order $\overline{\langle N\rangle}\log^2\overline{\langle N\rangle}$, both the thermal and the sample-to-sample distributions of the end-to-end distance are sharply peaked. We suspect that in the low-temperature phase the themal as well as the sample-to-sample fluctuations are $O(\overline{\langle N\rangle})$, and that in the high temperature phase the sample-to-sample fluctuations are negligible, as $\overline{\langle N\rangle}\to\infty$, compared to the thermal fluctuations.

7. Summary and perspectives

The spiralling self-avoiding walk on a square lattice with independent energy variables on each link may be studied through a simplified model. This model is expressed in terms of occupation variables of the lattice by the segments of the spiral.

The system exhibits a phase transition after rescaling the temperature and the distance with the mean number of steps of the walk, $\overline{\langle N\rangle}$, as $\overline{\langle N\rangle}^{1/4}$ and $\overline{\langle N\rangle}^{1/2}$ respectively. The occupation numbers of the simplified model have a Fermi distribution. This defines a Fermi level up to which all energy levels are filled at zero temperature. An order parameter characterizing the phase transition is defined in section 4. It gives the fraction of all segments, far from the origin, that are trapped at low energy levels. In the low temperature phase the walk is localized in these low energy regions. In the high temperature phase the walk behaves qualitatively as on a homogeneous lattice.

Furthermore, one can construct a spin glass picture where the walk defines a set of nested contours on a lattice of Ising spins. The correlation between two spins undergoes random sign changes on the temperature axis. In section 5 one sees that the density of sign changes diverges linearly with the distance between the two spins. This chaotic behaviour is present above as well as below the critical temperature. It

implies that a small temperature change necessitates important rearrangements of the walk segments. Above criticality such rearrangements will be physically brought about by thermal agitation. Below criticality, the correlation length (although never infinite in the present model) increases without bound as the temperature goes down. On a spatial scale less than the correlation length the system is frozen, and will not be able to carry out the rearrangements required by a temperature change. This will manifest itself experimentally in extremely slow relaxation, aging, etc.

The end-to-end distance of the set of segments was shown to be proportional to $\overline{\langle N\rangle}^{1/2}\log\overline{\langle N\rangle}$, as in the homogeneous case. However, there is a temperature dependent prefactor which becomes larger as the temperature is lowered. Hence the disorder increases the size of the walk, just as it does for a directed walk.

One of the remaining question is to develop the analogy, pointed out in section 4.4, of our model with the random energy model. The REM has a low temperature phase with many coexisting pure states. One may therefore ask if pure states can be distinguished also in the spiral SAW model, ask how many there are, and what their energy and overlap distributions are. Similar questions were investigated recently by Mézard [6] for the case of the directed walk.

Acknowledgment

We are indebted to M J A M Brummelhuis for the analysis of the function $\Phi(z)$ in appendix A.

Appendix A. The functions $\Phi(z)$ and $m(b)$

We analyse the function $\Phi(z)$ defined by (3.5). Upon replacing the integration variable u by $s\equiv y+u\sqrt{y}$, interchanging the two integrations, and setting $y\equiv t^2$ one obtains

$$\begin{aligned}\Phi(z)&=\sqrt{\frac{2}{\pi}}\int_{-\infty}^{\infty}\frac{\mathrm{d}s\,\mathrm{e}^{s}}{1+\mathrm{e}^{zs}}\int_{0}^{\infty}\mathrm{d}t\,t^{2}\exp\left(-\tfrac{1}{2}t^{2}-\frac{z^{2}}{2t^{2}}\right)\\&=\int_{-\infty}^{\infty}\mathrm{d}s\frac{(1+|s|)\,\mathrm{e}^{s-|s|}}{1+\mathrm{e}^{zs}}\\&=\int_{0}^{\infty}\mathrm{d}s\frac{1+s}{1+\mathrm{e}^{zs}}+\int_{0}^{\infty}\mathrm{d}s\frac{(1+s)\,\mathrm{e}^{-2s}}{1+\mathrm{e}^{zs}}\end{aligned}\tag{A1}$$

where, in the second step, we used [9], equation 3.472.2. By differentiating the last line of (A1) one shows that

$$\Phi'(z)<0\tag{A2a}$$

$$\Phi''(z)>0.\tag{A2b}$$

The first of the integrals in (A1) may be evaluated with the aid of [9], equations 3.311.1 and 3.411.3. The second one can be transformed with the aid of [9], equations 3.311.2 and 3.411.8. As a result one obtains

$$\Phi(z)=\frac{\pi^{2}}{12z^{2}}+\frac{\log 2}{z}+\sum_{k=0}^{\infty}\frac{(-1)^{k}}{2+kz}+\sum_{k=0}^{\infty}\frac{(-1)^{k}}{(2+kz)^{2}}.\tag{A3}$$

The series converge for all $z \geqslant 0$. It follows in particular that

$$\Phi(z) \simeq \frac{\pi^2}{12z^2} \qquad \text{as } z \to 0 \tag{A4a}$$

$$\Phi(1) = 2 \tag{A4b}$$

$$\Phi(\infty) = \tfrac{3}{4}. \tag{A4c}$$

We turn now to the function $m(b)$, which is the solution of (3.7). By combining this equation with (A4a) and (A4c) one readily finds

$$m(b) \simeq \frac{\pi}{2\sqrt{3}b} \qquad \text{as } b \to 0 \tag{A5a}$$

$$m(\infty) = (\tfrac{3}{4})^{1/4} J. \tag{A5b}$$

One may convince oneself graphically that $m(b)$ is monotonously decreasing. To show this analytically, we differentiate (3.7) with respect to b, which gives

$$\frac{\mathrm{d}m}{\mathrm{d}b} = -\frac{4bJ^6}{m^5} \Phi'\left(\frac{bJ^2}{m^5}\right)\left(\frac{\mathrm{d}m}{\mathrm{d}b} - \frac{m}{b}\right). \tag{A6}$$

This shows that $\mathrm{d}m/\mathrm{d}b$ cannot vanish for $0 < b < \infty$ and hence, in view of (A2a), is of a single sign. But this sign can be read off from (A5a), and therefore

$$m'(b) < 0 \tag{A7}$$

for all b.

Appendix B

In this appendix, we obtain the occupation probability $\langle n(r) \rangle$ averaged on the disorder, in the large-r limit,

$$\overline{\langle n(r) \rangle} = \int_{-\infty}^{\infty} \frac{\mathrm{d}u}{\sqrt{2\pi}} \mathrm{e}^{-\frac{1}{2}u^2} \frac{1}{1 + \mathrm{e}^{bm(b)r + b\sqrt{r}\,u}}. \tag{B1}$$

The integrand in (A1) is a Gaussian multiplied by a Fermi distribution. For large r it is a function with a sharp peak. The energy at which the peak is located, called u^*, is negative. We shall see how it depends on the temperature (through b). We will find two results for $\overline{\langle n(r) \rangle}$ and two corresponding regimes of temperature.

After the transformation $v \equiv mr + \sqrt{r}\,u$ in (B1), one finds

$$\overline{\langle n(r) \rangle} = \frac{\mathrm{e}^{-(m^2/2)r}}{\sqrt{r}} \int_{-\infty}^{\infty} \frac{\mathrm{d}v}{\sqrt{2\pi}} \frac{\mathrm{e}^{vm}}{1 + \mathrm{e}^{vb}} \mathrm{e}^{-v^2/2r}. \tag{B2}$$

One can expand the exponential $\mathrm{e}^{-v^2/2r}$ in the large-r limit. For reasons of convergence, one easily sees that this expansion is allowed if and only if

$$m(b) < b \tag{B3}$$

that is, in a regime of low temperature. In that case, the result is to leading order

$$\overline{\langle n(r) \rangle} \simeq \frac{\mathrm{e}^{-(m^2/2)r}}{\sqrt{2\pi r}} \int_{-\infty}^{\infty} \frac{\mathrm{e}^{mv}}{1 + \mathrm{e}^{bv}} \qquad r \gg 1 \tag{B4}$$

where the integral may be evaluated with [9], equation 3.311.9 and gives (4.4*c*). Hence, for $m(b) < b$, the integrand in (B1) has a peak at

$$u^*(b) = -m(b)\sqrt{r} \tag{B5}$$

with a width $\Delta u^*(b)$ which is of order $1/\sqrt{r}$.

Let us now consider the remaining high temperature regime,

$$m(b) > b. \tag{B6}$$

We expand the integrand in (B.1) in powers of $\exp[-bmr - b\sqrt{r}u]$ and get leading order

$$\overline{\langle n(r)\rangle} \simeq \int_{-\infty}^{\infty} \frac{du}{\sqrt{2\pi}} e^{-u^2/2} e^{-bmr - b\sqrt{r}u} = e^{-(bm - b^2/2)r} \qquad r \gg 1. \tag{B7}$$

Here we have $u^* = b\sqrt{r}$, and $\Delta u^*(b)$ is of order one. Each of the results (B4) and (B7) is the first term of an asymptotic expansion that can be completely determined if necessary.

References

[1] Privman V 1983 *J. Phys. A: Math. Gen.* **16** L571
[2] Blöte H W J and Hilhorst H J 1984 *J. Phys. A: Math. Gen.* **17** L111
[3] Guttmann A J and Wormald N C 1984 *J. Phys. A: Math. Gen.* **17** L271 3614
Joyce G S 1984 *J. Phys. A: Math. Gen.* **17** L463
[4] Guttmann A J and Hirschhorn M 1984 *J. Phys. A: Math. Gen.* **17** 3613
Guttmann A J and Wallace K J 1985 *J. Phys. A: Math. Gen.* **18** L1049
Whittington S G 1985 *J. Phys. A: Math. Gen.* **18** L67
Joyce G S and Brak R 1985 *J. Phys. A: Math. Gen.* **18** L293
Lin K Y 1985 *J. Phys. A: Math. Gen.* **18** L145
Liu K C and Lin K Y 1985 *J. Phys. A: Math. Gen.* **18** L647
Liu K C, Chiu S H, Ma S K and Kao C H 1986 *J. Phys. A: Math. Gen.* **19** 3093
Szekeres G and Guttmann A J 1987 *J. Phys. A: Math. Gen.* **20** 481
[5] Huse D A and Henley C L 1985 *Phys. Rev. Lett.* **54** 2708
Kardar M 1985 *Phys. Rev. Lett.* **55** 2923
Huse D A, Henley C L and Fisher D S 1985 *Phys. Rev. Lett.* **55** 2924
Zhang Y C 1987 *Phys. Rev. Lett.* **59** 2125
Nattermann T 1988 *Phys. Rev. Lett.* **60** 2701
Derrida B and Golinelli, O 1990 *Phys. Rev.* A **41** 4160
[6] Mézard M 1990 *J. Physique* **51** 1831
[7] Derrida B 1981 *Phys. Rev.* B **24** 2613
[8] Kirkpatrick S and Sherrington D 1978 *Phys. Rev.* B **17** 4384
Sherrington D 1980 *J. Phys. A: Math. Gen.* **13** 637
[9] Gradshteyn I S and Ryzhik I M 1965 *Tables of Integrals, Series and Products* (New York: Academic)
[10] Fisher D S and Huse D A 1986 *Phys. Rev. Lett.* **56** 1601
Bray A J and Moore M A 1987 *Phys. Rev. Lett.* **58** 57
Nifle M and Hilhorst H J 1991 *J. Phys. A: Math. Gen.* **24** 2397